Reversible nonmagnetic single-photon isolation using unbalanced quantum coupling

Keyu Xia (夏可宇),[1,*] Guowei Lu,[2] Gongwei Lin,[3] Yuqing Cheng,[2] Yueping Niu,[3] Shangqing Gong,[3] and Jason Twamley[1]

[1]*ARC Centre for Engineered Quantum Systems, Department of Physics and Astronomy, Macquarie University, NSW 2109, Australia*

[2]*State Key Laboratory for Mesoscopic Physics, Department of Physics, Peking University, Beijing 100871, China*

[3]*Department of Physics, East China University of Science and Technology, Shanghai 200237, China*

(Received 27 May 2014; published 1 October 2014)

The nonreciprocal propagation of light at the single-photon level is essential for building a quantum network. Bulk optical schemes are lossy and difficulty to integrate onto a chip. We propose a single-photon optical diode and a three-port circulator without a magnetic field by coupling an unbalanced quantum impurity to a passive, linear optical waveguide or a whispering-gallery-mode microresonator which supports a locally or globally circularly polarized photon. Thanks to the unbalanced quantum Jaynes-Cummings coupling, the optical nonreciprocal propagation of single photons can be achieved without an external magnetic field. In particular, the three-port single-photon circulator can be accomplished using the existing experimental technology. The optical isolation can be reversed by selectively populating the initial state of the quantum impurity. Moreover, by using an ensemble of identical atoms filled in a hollow-core microbottle resonator, nonreciprocal propagation of weak light pulses can be achieved.

DOI: 10.1103/PhysRevA.90.043802 PACS number(s): 42.50.Pq, 42.25.Bs, 42.50.Ex, 42.82.Et

I. INTRODUCTION

On-chip optical nonreciprocal propagation, e.g., optical isolation, has attracted intensive research [1–11] for its important potential applications in optical communications and technology. The development of nonreciprocal optical devices is a longstanding but highly challenging goal in integrated optics. In bulk optics, this is achieved using the Faraday effect. Despite many attempts, on-chip devices using the magneto-optical effect [1,2], optical nonlinearity [3,4], and photonic crystal heterojunctions [5] may suffer large losses in transmission. A nearly unit transmission can be achieved via the modulation of the material's optical properties temporally and in space [6–8], or by using a parametric process [9,10]. The breaking of parity-time symmetry has been used to demonstrate optical nonreciprocity [12,13]. However, these schemes are not suitable for a single-photon diode because the field at the single-photon level is too weak for an optical nonlinear process.

A single photon is a vital resource for quantum information processing. The unidirectional propagation of a single photon is therefore crucial for many quantum applications, such as constructing a quantum internet [14,15], but achieving such unidirectional photon transport at the quantum level remains a difficult and so-far-unsolved problem. The only two works towards this direction are proposed by Shen *et al.* using local photon polarization in a photonic crystal waveguide [16], and by Hafezi and Rabl using an optomechanical resonator [17].

In this paper, we show that all-solid-state single-photon isolation without an external magnetic field can be achieved with a near unit contrast by exploiting an unbalanced quantum impurity, e.g., cesium atoms coupled to a passive, linear photonic circuit. Unlike the use of weak optical nonlinearity, or using temporal modulation or the Faraday effect, our magnetic-field-free configuration is here based on cavity quantum electrodynamics, which can work at the single-photon level and can be integrated on a chip. This scheme will also work for a weak signal light as long as we use an ensemble. Although cavity-QED setups have been previously studied for the control of photons by adding or removing a single Rb atom to high-Q optical whispering gallery modes (WGMs) [18,19], the important application of nonreciprocal behavior for photon circulators has not been fully addressed, in particular, the photon circulator at the single-photon level. We also note that although Witthaut and Sørensen discussed quantum interference by a V-type emitter in a one-dimensional waveguide [20], nonreciprocal behavior was not addressed.

II. SYSTEM

Here we first explain the basic idea for our optical isolation. We dope a V-type quantum impurity with degenerate transition frequencies ω_q, but different dipole moments $\mu_\pm$, and decay rates $\gamma_\pm$ at a certain place where a passive, linear waveguide or WGM microresonator couples to it. Essentially different from Shen's work [16], the quantum impurity in our scheme couples to the σ_+- and σ_--polarized light with different rates, $g_+ \propto \mu_+$ and $g_- \propto \mu_-$, respectively. The waveguide [16] or WGM microresonator [18,19,21] supports a locally or globally planar, circular polarization. In such optical setups the polarization of the light is dependent on the propagation direction of the light. For instance, one can arrange that the polarization of light at the location of the impurity is right-hand circular (σ_+) when the input light propagates forward (left-hand input), while it is σ_- polarized for the backward-propagating photon (right-hand input). As a result, *time reversal symmetry breaks if* $|g_+| \neq |g_-|$, leading to the nonreciprocal propagation of a single-photon even without an external magnetic field. We go further to study a WGM microresonator mentioned above coupled to a bus(throughput) waveguide and a drop waveguide simultaneously. Such a configuration constitutes a three-port single-photon circulator.

Now we start by describing the configuration of our single-photon diode and circulator. We propose two implementations for the single-photon diode and one for the photon circulator.

*keyu.xia@mq.edu.au

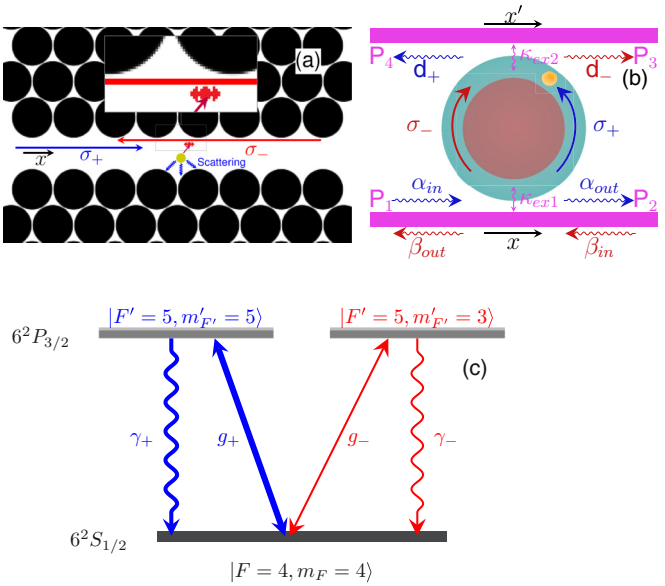

FIG. 1. (Color online) Schematics of the single-photon diode and circulator. (a) Single-photon diode using an unbalanced quantum impurity implanted at the center (zoomed view) of a photonic crystal line-defect waveguide (white) with triangular lattice of air holes (black). The zoomed insert view shows the position where the waveguide possesses locally circular polarization. The polarization at this central location is found to be circular by a numerical finite-difference time-domain (FDTD) simulation for $\lambda = 852$ nm. This wavelength is tunable by tuning the size of air holes. The σ_--polarized photons entering from the right are transmitted because they mostly decouple from the quantum impurity, while σ_+-polarized photons incident from the left are scattered by the impurity into the open environment due to the considerable large coupling. (b) Single-photon diode or circulator using an unbalanced quantum impurity doped in a WGM microresonator with resonance frequency ω_c. The microresonator possesses locally [21] or globally [18,19] a right-circular-polarized (σ_+ -polarized) counterclockwise mode and a left-circular-polarized (σ_--polarized) clockwise one. The cavity couples to a lower bus (throughput) waveguide with a rate κ_{ex1} and a upper drop waveguide with a rate κ_{ex1}. (c) A Cs atom working as a unbalanced quantum impurity with $g_+ \gg g_-$ and decay rates $\gamma_+ \gg \gamma_-$ [22]. In both branches, the transition frequencies are ω_q. The Cs atom can also be replaced with a Rb atom [18,19] or a quantum dot [23].

The type-I single-photon diode can be modeled as the single-photon transport in a line-defect waveguide [Fig. 1(a)]. The waveguide is a single-polarized single mode (SPSM) waveguide possessing either a right-hand circular polarized (σ_+) light or a left-hand circular polarized (σ_-) light. The type-II single-photon diode and circulator are based on cavity QED involving a WGM microresonator [Fig. 1(b)]. In this setup, the left-hand linear polarized pump light excites a σ_+-polarized counterclockwise mode, whereas the right-hand input drives a σ_--polarized clockwise mode [18,19,21]. In both cases, the doped quantum impurity strongly couples to the σ_+-polarized light but weakly interacts with the σ_- polarization [18,19,21]. As a consequence, the time-reverse symmetry of the whole system breaks. The single-photon diode shown in Fig. 1(a) permits optical nonreciprocity so that the system scatters the left-hand input single photons into an open environment but behaves transparently for the right-hand input photons. In Fig. 1(b), we construct a three-port single-photon circulator. When the photon inputs into the port P_1, it comes out from the port P_2. Interestingly, the photons incident to the port P_2 transport to the third port P_3. Therefore, this configuration forms a single-photon circulator. The type-II single-photon diode is a specific case of circulator if we remove the drop waveguide. Throughout our investigation below, we use a Cs atom as the quantum impurity so that $\mu_+ = \sqrt{45}\mu_-$ and $r = |\mu_+|/|\mu_-|^2 = 45$ [22]. The parameter μ_- can be completely suppressed by using a negatively charged quantum dot [23] and subsequently r can be enhanced by orders of magnitude.

III. PHOTONIC CRYSTAL CONFIGURATION

The first configuration in Fig. 1(a) can only work as an optical diode. Note that the quantum emitter scatters the σ_+-polarized photons from the left into open environment but does not reflect it back to the right. There are two reasons: First, we assume that the quantum emitter is doped at the position where the waveguide ideally possesses only the right-propagating σ_+ polarization photons or the left-propagating σ_- polarization photons, while the left-propagating σ_+ polarization photons are completely suppressed. Secondly, the excited emitter by the σ_+ polarization photons can only emit the right-propagating mode or scatter photons into an open environment. Therefore, the reflection of the σ_+-polarized photons should always be zero ideally. We can derive the steady-state solution for the transmission for the two atomic transitions by using the photon transport method [16,24] (see Appendix A),

$$t_\pm(\omega) = \frac{\omega - \omega_q - i(\gamma_\pm - \Gamma_\pm)}{\omega - \omega_q + i(\gamma_\pm + \Gamma_\pm)}, \tag{1}$$

where ω is the carrier frequency of the input photon and $\Gamma_\pm = V_\pm^2/2v_g$, $V_\pm$ is proportional to the dipole moments, $\mu_\pm$ is the coupling strength between the field in the waveguide and the quantum impurity, and v_g is the group velocity of the photon in the waveguide. Because $\mu_+ \gg \mu_-$ and $\gamma_\pm, \Gamma_\pm \propto |\mu_\pm|^2$, the ratio $r = \gamma_+/\gamma_- = \Gamma_+/\Gamma_- \gg 1$. The transmission is defined as $T_\pm = |t_\pm|^2$ and $R_\pm = |r_\pm|^2$, respectively. Obviously, the transmission disappears only at the on-resonance critical coupling, i.e., $\omega - \omega_q = 0$ and $\gamma_\pm = \Gamma_\pm$. The contrast is evaluated as $\eta = |T_- - T_+|/|T_- + T_+|$ [16]. The detuning is defined as $\Delta = \omega_q - \omega$.

We set $\alpha = \Gamma_+/\gamma_+ = \Gamma_-/\gamma_-$, which is the ratio of atomic dissipation rates due to the coupling of the emitter to the waveguide and open environment. If $\alpha \approx 1$, the doped quantum impurity can create nonreciprocal windows, as shown in Fig. 2. It can be clearly seen that T_- is almost equal to unity for a right-hand input, while T_+ is small if $10 \leqslant |\Delta|/\gamma_- \leqslant 30$. The resulting contrast η is larger than 0.80. Note that two transmissions T_+ and T_- are the same, ~ 0 at $\Delta = 0$ for both of the right-handed and left-handed inputs. At vanishing detuning, irrespective of the input port, propagation through the waveguide is greatly restricted [see Fig. 2(a)]. However, the linewidths of the dip for the left-hand input (blue solid line) are much broader than those for the right-handed incident photon (red dashed line). As a result of this directionality-dependent

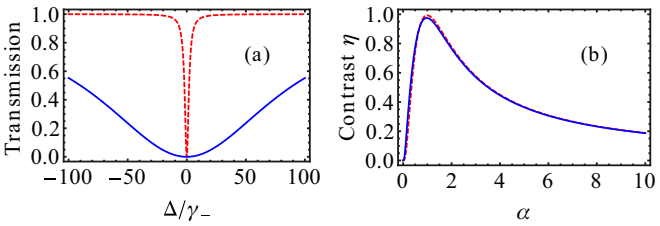

FIG. 2. (Color online) (a) Steady-state transmission of the type-I single-photon diode [Fig. 1(a)] as a function of Δ at $\alpha = 1$. Solid blue line is for the transmission T_+, while the dashed red line is for T_-. (b) Contrast as a function of α. Solid blue line indicates η for $\Delta/\gamma_- = 10\alpha$ and the dashed red line for $\Delta/\gamma_- = 5\alpha$. The two lines mostly overlap. η is larger than 0.8 when $0.53 < \alpha < 1.8$.

linewidth, a single-photon wave packet with a duration $\Gamma_+^{-1} \ll \tau \ll \Gamma_-^{-1}$ when incident from the right is mostly transmitted to output to the left, while if it is incident from the left it is mostly scattered away to the open environment.

The contrast α is an important parameter affecting the performance of the single-photon diode, which makes use of the coupling of a single quantum impurity to a line-defect waveguide. It can be clearly seen from Fig. 2(b) that a good nonreciprocal behavior occurs only around the critical coupling $\alpha \sim 1$. Correspondingly, the contrast η can be larger than 0.8 if $5\alpha \leqslant |\Delta|/\gamma_- \leqslant 10\alpha$ and $0.53 < \alpha < 1.8$.

IV. WGM MICRORESONATOR CONFIGURATION

Below we discuss the transmission to the bus and drop ports for the type-II single-photon diode and the circulator. We find that the two counterpropagating modes in the WGM microresonator couple to the quantum impurity with different coupling strengths due to the different dipole moments μ_+ and μ_-, as shown in Fig. 1(b). Similar to the type-I single-photon diode, the transmissions into the bus and drop waveguides are found to be given by (see Appendix B)

$$t_{\pm,B}(\omega) = 1 + \frac{2i\kappa_{ex1}}{\omega_c - \omega - i\kappa - \frac{|g_\pm|^2}{\omega_q - \omega - i\gamma_\pm}}, \tag{2a}$$

$$t_{\pm,D}(\omega) = \frac{2i\sqrt{\kappa_{ex1}\kappa_{ex2}}}{\omega_c - \omega - i\kappa - \frac{|g_\pm|^2}{\omega_q - \omega - i\gamma_\pm}}, \tag{2b}$$

where $\kappa_{ex1}(\kappa_{ex2}) = V_1^2/2v_g(V_2^2/2v_g)$ is the decay rate of the cavity due to the external coupling $V_1(V_2)$ to the bus (drop) waveguide, and $\kappa = \kappa_i + \kappa_{ex1} + \kappa_{ex2}$ is the total decay rate of the cavity where κ_i is the intrinsic decay rate of the cavity. We define the detuning $\Delta = \omega_c - \omega$ and always assume that $\omega_c = \omega_q$, the degenerate internal transition frequency of the V-type atom. The transmissions are defined as $T_{\pm,B} = |t_{\pm,B}|^2$ and $T_{\pm,D} = |t_{\pm,D}|^2$. We assume that the photons in both of the bus and drop waveguides have the same group velocity v_g.

A. Type-II single-photon diode

The type-II single-photon diode is a specific case of the circulator when $\kappa_{ex2} = 0$. As a result, $T_{\pm,D} = 0$. In this case, the cavity works as a single-photon diode, as shown in Fig. 3. For simplicity, we substitute $T_{\pm,B}$ with $T_\pm$ here. If $g_- = 0$ and $g_+ \gg \kappa_i$, $\Delta \approx 0$, the forward transmission is 1, $T_+ = 1$, while $T_- \approx 0$. This can be achieved using a negatively charged quantum dot [23]. If, however, $|g_-| > 0$ and $\Delta \approx 0$, the nonreciprocal window disappears. However, for $|\Delta| \approx |g_-|$, $\gamma_+ = 0$, and $g_+/\kappa_i \gg 1$, only the right-moving photon can pass through the cavity, $T_+ = 1$ (solid blue line), while the left-moving photon decays into the environment via the cavity, $T_- = 0$ (solid red line). At $|\Delta| = |g_+|$, the optical nonreciprocity reversed. The device is transparent for the left-moving photon but blocks the right-moving photon. If $\gamma_+ \gg \kappa_i$ (dotted green line), part of the excitation of the right-moving photon can pass through the device.

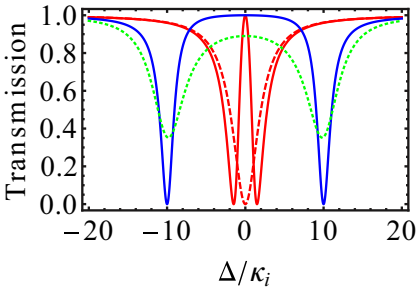

FIG. 3. (Color online) Steady-state transmissions of the type-II single-photon diode using the WGM microresonator [Fig. 1(b)] in the absence of the drop waveguide, i.e., $\kappa_{ex2} = 0$, and under the critical coupling condition $\kappa_{ex1} = \kappa_i$. Dashed and solid red lines show the transmission T_- when $g_- = 0$ and $g_- = g_+/\sqrt{45}$, while solid-blue and dotted-green lines are for the transmission T_+ when $\gamma_+ = 0$ and $\gamma_+ = 3\kappa_i$, respectively. $g_+ = 10\kappa_i$.

B. Single-photon circulator

To construct a single-photon circulator, we add a drop waveguide to the device and both of the bus and drop waveguides overcouple to the cavity, e.g., $\kappa_{ex1} = \kappa_{ex1} = 3\kappa_i$ [see Fig. 4(a)]. We are interested in the vicinity of $\Delta \sim 0$. For the left-hand input α_{in}, most excitation of the photon can transport to the bus-waveguide port P_2, $T_{+,B} = 0.85$ (solid blue line), and the output to the drop port P_4 (dashed blue line)

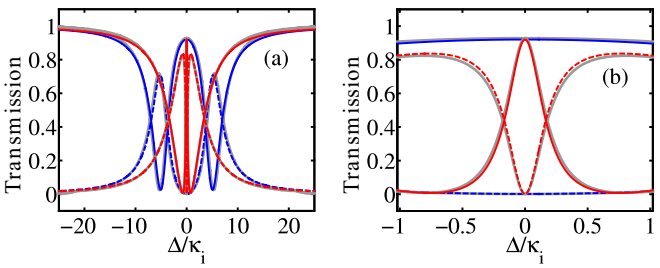

FIG. 4. (Color online) Nonmagnetic single-photon circulator by coupling an unbalanced quantum impurity to a WGM microresonator. (b) The zoom in of (a). Solid blue (red) line shows the direct transmission $T_{+,B}$ ($T_{-,B}$) in the bus waveguide, while the dashed blue (red) line shows the transmission $T_{+,D}$ ($T_{-,D}$) in the drop waveguide. The gray lines (almost overlapping with the other lines) are the results from numerical simulations of Eq. (3). $g_+ = 5\kappa_i$, $g_- = g_+/\sqrt{45}$, $\gamma_+ = 0.3\kappa_i$, $\gamma_- = \gamma_+/45$, and $\kappa_{ex1} = \kappa_{ex2} = 3\kappa_i$.

is vanishingly small. The transmission for the right-hand input is more complicated. There is a dip (peak) in the transmission $T_{-,D}$ ($T_{-,B}$), but the linewidth is very small, about $0.16\kappa_i$ [Fig. 4(b)]. In contrast, the whole transmission profile has a linewidth of $11\kappa_i$. Therefore, a single-photon pulse with a finite bandwidth $0.16\kappa_i \ll \Delta B \ll 11\kappa_i$ can transport to the drop port P_3 with a probability of 74%. The probability transmitting to the bus-waveguide port P_1 is small, about 2%, yielding a contrast 0.95. However, the performance of the isolation needs to be evaluated by numerically simulating the propagation of a single-photon pulse, as in the case of the photon storage [25]. Our numerical simulations match the analytic forms well (see gray lines in Fig. 4). If $|\Delta| \sim g_-$, the nonreciprocal behavior of the circulator is clear, $T_{+,B} = 0.835$ to the port P_2, $T_{+,D} = 0.032$ to P_4, and $T_{-,B} = 0.021$ to the port P_1, $T_{-,D} = 0.733$ to P_3. As a result, the device forms a $P_1 \to P_2 \to P_3$ circulator with ports P_1, P_2, and P_3. The single-photon incident from the port P_1 transmits to the port P_2, while the photon entering the port P_2 comes out from the port P_3.

However, the isolation of a long single-photon pulse when $|\Delta| = g_-$ can be clearly seen from Fig. 4. The dynamics of the single photon around $\Delta \sim 0$ is complicated.

To provide a numerical proof of the single-photon isolation using the circulator, we numerically simulated the propagation of a single-photon pulse in time as it passed through the circulator. To do so, we numerically solved the following set of equations of motion:

$$i\partial_t \phi_{\pm,B}(x,t) = \pm i v_g \partial_x \phi_{\pm,B}(x,t) + V_1 \delta(x) e_c, \quad (3a)$$

$$i\partial_t \phi_{\pm,D}(x',t) = \mp i v_g \partial'_x \phi_{\pm,D}(x',t) + V_2 \delta(x') e_c, \quad (3b)$$

$$i\partial_t e_c = (\Delta - i\kappa_i) e_c + V_1 \phi_{\pm,B}(x,t)\delta(x) + V_2 \phi_{\pm,D}(x',t)\delta(x') + g^*_{\pm} e_a, \quad (3c)$$

$$i\partial_t e_a = (\Delta - i\gamma_{\pm}) e_a + g_{\pm} e_c, \quad (3d)$$

where $\phi_{\pm,B}(x,t)$ ($\phi_{\pm,D}(x',t)$) is the wave function of the traveling photon at x (x') in the bus (drop) waveguide for the left-hand (right-hand) input. e_c is the excitation of the counterclockwise (clockwise) cavity mode corresponding to the the left-hand (right-hand) input, and e_a is the excitation in the σ_+ (σ_-) transition branch of the quantum impurity.

We input a Gaussian pulse wave packet, $\phi(x,0)_{\pm,B} = \sqrt[4]{\tau^2/\pi} e^{-(x-x_0)^2/2\tau^2}$, where τ is the spatial duration of the pulse. The input is normalized to yield a single excitation, $\int_{-\infty}^{+\infty} \phi^*(x,0)\phi(x,0)dx = 1$. Figure 5 shows the wave packets of photons at the same time t_d for the left and right input. The transmissions are evaluated by $T_{\pm,B/D} = \int_{-\infty}^{+\infty} \phi^*_{\pm,B/D}(x,t_d)\phi(x,t_d)dx$ to be $\{T_{+,B}, T_{-,B}, T_{+,D}, T_{-,D}\} = \{0.9, 0.178, 0.02, 0.675\}$ excitations outgoing to the port $\{P_2, P_1, P_4, P_3\}$. Clearly, a three-port circulator at the single-photon level is achieved.

V. DISCUSSION AND CONCLUSION

So far, we assume that $\mu_+ \gg \mu_-$. Note that $\mu_+ \ll \mu_-$ if we initially populate the state $|6\,^2S_{1/2}, F = 4, m = -4\rangle$ for Cs atoms or $|5\,^2S_{1/2}, F = 3, m = -3\rangle$ for Rb atoms. Therefore, the optical nonreciprocity can be reversed, and the configuration in Fig. 1(b) forms a $P_2 \to P_1 \to P_4$ circulator. The atom can be implanted into the microresonator to form a solid-state device [26], or the atom can be also substituted by a negative-charged quantum dot [23]. Our reversible nonmagnetic single-photon diode or circulator can be realized using existing technology. For instance, the intrinsic decay rate of a WGM microresonator possessing a globally circular polarization can reach $\kappa_i = 4.8$ MHz [19]. A single Cs or Rb atom close to the surface of the microresonator can interact with a cavity mode with a strength $g_+/2\pi = 17 - 50$ MHz [18,19,22,27]. The dissipation rate of the Cs atom is measured to be $\gamma_+/2\pi \approx 2.5$ MHz. For the Cs atom, $\mu_+ = \sqrt{45}\mu_-$, yielding $g_+ = \sqrt{45}g_-$ and $\gamma_+ = 45\gamma_-$. The external coupling κ_{ex1} and κ_{ex2} can be turned to $\sim$20 MHz[18,19]. Thus the circulator can be implemented based on these parameters.

We use the single-photon transport model in real space developed by Shen and Fan [24] for our numerical simulation. This single-photon transport model governs the interaction of a single photon and a quantum emitter. It has been widely used to study the time dynamics [28], the frequency conversion [29,30], and the steady-state transmission [20,31,32] of a single photon in real space. This single-photon transport model considers at most one excitation in the Hilbert space. It neglects the vacuum state, which has zero photons, and has the atom in the ground state, and also truncates the higher excitation states. Thus, the shape of the general stationary state and the time evolution equation (3) are scalable in mathematics. The model is valid for a single-photon input in the single-excitation space. However, this single-photon transport model cannot be simply applied to a coherent state scattering problem because the model is valid only for the single-excitation Hilbert space. To evaluate the performance of our devices, we normalize the total (input) excitation to unitary. Actually, the method can be extended to investigate few-photon transport in real space [33–37], but the general eigenstates and the evolution equation need to change accordingly to include higher excitation states in Hilbert space.

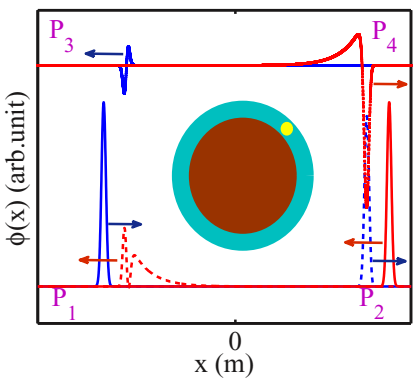

FIG. 5. (Color online) Propagation of single-photon pulses with $\sim 4\kappa_i$ in the circulator for $\Delta = 0$ and $v_g = 1 \times 10^8$ m/s, as in Fig. 4. The cartoon circles indicate the cavity and the quantum impurity, respectively. The arrows indicate the moving directions. Blue (red) lines show the input and transmitted field for the left-hand (right-hand) input.

Although this work studies the single-photon isolation, it can be extended to isolate a weak coherent laser pulse spanning a broadband if we envisage a hollow bottle microresonator using a hollow-core optical fiber [38] filled with Rb or Cs atom vapor [39–41]. The atoms close to the inner surface of a microresonator strongly couple to the cavity mode and the collective coupling is enhanced by $\sqrt{N}$, yielding a rate $\sqrt{N}g_+$, where N is the number of total involved atoms. This collective coupling can reach several gigahertz, since g_+ can be ~50 MHz. Furthermore, such a design (gas atoms inside a hollow WGM resonator) is able to provide a single photon or weak-pulse photon isolation to work for photon isolation at room temperature [39,40,42]. Therefore, our optical isolator can work at room temperature and allow a unidirectional transport of photons with a speed of gigahertz.

In conclusion, we have studied the optical nonreciprocity induced by the unbalanced coupling between a V-type quantum impurity and a single photon. We have proposed two schemes for the single-photon diode and one scheme for the single-photon circulator. Interestingly, the nonreciprocal optical device without external magnetic fields can be integrated in a passive, linear photonic circuit. In particular, the single-photon three-port circulator can be a building block for a quantum internet [14,15]. Furthermore, the optical nonreciprocity can be reversed by manipulating the initial state of the quantum impurity.

ACKNOWLEDGMENTS

This work was funded by the Australian Research Council Centre of Excellence for Engineered Quantum Systems (EQuS), CE110001013, and the National Natural Science Foundation of China (Grants No. 11204080, No. 11274112, and No. 61275215).

APPENDIX A: TYPE-I SINGLE-PHOTON DIODE

In this Appendix, we derive the steady-state transmission for each type of diode and the circulator using the photon transport method developed by Shen and Fan [24]. Given the Hamiltonian $\hat{H}$ describing the motion of system with eigenstate $|\psi\rangle$, we have the Schrödinger equation $i\frac{\partial|\psi\rangle}{\partial t} = \hat{H}|\psi\rangle$. Below we start from the Schrödinger equation to derive the steady-state transmission and reflection.

For the single-photon diode using the photonic crystal linear defect, the Hamiltonian in real space describing the interaction of the quantum impurity and the traveling single photon is given by

$$\begin{aligned}\hat{H} = &\int dx\left[\hat{C}_R^\dagger\left(\omega_{\rm in} - iv_g\frac{\partial}{\partial x}\right)\hat{C}_R\right.\\ &\left.+\hat{C}_L^\dagger\left(\omega_{\rm in} + iv_g\frac{\partial}{\partial x}\right)\hat{C}_L\right]\\ &+V_\pm\int dx\delta(x)[\hat{S}_+\hat{C}_R + \hat{C}_R^\dagger\hat{S}_- + \hat{S}_+\hat{C}_L + \hat{C}_L^\dagger\hat{S}_-]\\ &+(\omega_e - i\gamma_\pm)\hat{a}_e^\dagger\hat{a}_e + \omega_g\hat{a}_g^\dagger\hat{a}_g, \end{aligned}\tag{A1}$$

where $\hat{C}_R^\dagger[\hat{C}_L^\dagger]$ is a bosonic operator creating a right-going (left-going) photon at x. $\hat{a}_g^\dagger(\hat{a}_e^\dagger)$ is the creation operator of the ground (excited) state of the atom, and $\omega_e - \omega_g = \omega_q$. The excited states are $|F' = 5, m'_{F'} = 5\rangle$ for the σ_+ driving and $|F' = 5, m'_{F'} = 3\rangle$ for the σ_- driving. $\hat{S}_+ = \hat{a}_e^\dagger\hat{a}_g$ and $\hat{S}_- = \hat{S}_+^\dagger$. $V_\pm$ is proportional to the dipole moments, $\mu_\pm$ is the coupling strength between the field in the waveguide and the quantum impurity, and v_g is the group velocity of the photon in the waveguide. The first (second) term describes the free evolution of the right-going (left-going) mode. The second line shows the interaction between the quantum impurity and the traveling modes. The free Hamiltonian of the impurity is described by the last line.

We assume that the eigenstate of the system given by $|\psi\rangle = [\int dx\tilde{\phi}_R\hat{C}_R^\dagger + \int dx\tilde{\phi}_L\hat{C}_L^\dagger + \tilde{e}_a\hat{a}_e^\dagger\hat{a}_g]|\varnothing\rangle$ has the eigenvalue ω so that $\tilde{X} = e^{-i\omega t}X$ with $X \in \{\phi_R, \phi_L, e_a\}$. $\tilde{\phi}_R(x,t)$ and $\tilde{\phi}_L(x,t)$ are the wave functions of the right-moving and left-moving photons, respectively. $\tilde{e}_a(t)$ is the excitation of the quantum impurity. $|\varnothing\rangle$ is the vacuum state with zero photons in the waveguide and with the atom in the ground state. We assume that the quantum impurity locates at $x = 0$. For simplicity, we consider the ideal case that the field at the position of the quantum impurity is completely σ_+- or σ_--polarized. In this case, the σ_+ (σ_-)-polarized incident photon couples only to the σ_+ (σ_-) transition of the emitter. The emitter cannot generate σ_- (σ_+)-polarized photons and only scatters the photon into the environment. Therefore the reflection R for both the left- and right-hand input is always zero ideally. For the purpose solving the transmission amplitude for an incident photon, we have $\phi_R(x) = e^{iQx}[\theta(-x) + t_+\theta(x)]$ for a left-hand incident photon and $\phi_L(x) = e^{-iQx}[t_-\theta(-x) + \theta(x)]$ for a right-hand input for modes at location x [24], where $t_\pm$ is the transmission amplitude. $\theta(x)$ is the Heaviside step function that $\theta(x)|_{x=0} = 1/2$, $\frac{\partial\theta(x)}{\partial x}|_{x\to 0_+} = 1$ and $\frac{\partial\theta(-x)}{\partial x}|_{x\to 0_-} = -1$ [43,44]. Q is the wave vector of the input field around the frequency ω. In the vicinity of $\omega_{\rm in}$, we linearize the dispersion of the waveguide and have $Q = (\omega - \omega_{\rm in})/v_g$. As a result,

$$\begin{aligned}\phi_R(0) &= \frac{1+t_+}{2},\\ \phi_L(0) &= \frac{1+t_-}{2},\\ -iv_g\frac{\partial\phi_R(x)}{\partial x}|_{x=0} &= (\omega-\omega_{\rm in})\phi_R(0) - iv_g(t_+ - 1),\\ iv_g\frac{\partial\phi_L(x)}{\partial x}|_{x=0} &= (\omega-\omega_{\rm in})\phi_L(0) + iv_g(1 - t_-).\end{aligned}\tag{A2}$$

In the steady state, we have

$$(\omega - \omega_{\rm in})\phi_R(0) = -iv_g\partial_x\phi_R(x)|_{x=0} + V_+e_a, \tag{A3a}$$

$$(\omega - \omega_{\rm in})e_a = (\Delta - i\gamma_+)e_a + V_+\phi_R(0), \tag{A3b}$$

for a left-hand input, and

$$(\omega - \omega_{\rm in})\phi_L(0) = iv_g\partial_x\phi_L(x)|_{x=0} + V_-e_a, \tag{A4a}$$

$$(\omega - \omega_{\rm in})e_a = (\Delta - i\gamma_-)e_a + V_-\phi_L(0), \tag{A4b}$$

for a right-hand input.

Then we can derive the steady-state solution that for the transmission for the left (right)-hand incident σ_+ (σ_-) photon

driving the atomic σ_+ (σ_-) transitions by using the photon transport method [24,43,44]

$$t_\pm(\omega) = \frac{\omega - \omega_q - i(\gamma_\pm - \Gamma_\pm)}{\omega - \omega_q + i(\gamma_\pm + \Gamma_\pm)}, \tag{A5}$$

where $\Gamma_\pm = V_\pm^2/2v_g$. The transmission is defined as $T_\pm = |t_\pm|^2$, and the detuning $\Delta = \omega_q - \omega$.

APPENDIX B: TYPE-II SINGLE-PHOTON DIODE AND CIRCULATOR

In the configuration shown in Fig. 1(b), the unbalanced quantum impurity doped in a WGM microresonator couples to the σ_+-polarized counterclockwise mode and the σ_--polarized clockwise mode with different rates g_+ and g_-, respectively. The cavity overcouples to a bus waveguide and a drop waveguide with external coupling κ_{ex1} and κ_{ex2}, respectively. The laser inputting into the bus waveguide from the port P_1 (P_2) excites the counterclockwise mode (the clockwise mode). The transmitted pulses propagate in either the bus waveguide or the drop waveguide. When $\kappa_{ex2} = 0$ the circulator can be considered as a single-photon diode. In this specific case, the device without the drop waveguide works as a type-II single-photon diode.

Here we discuss the transmission to the bus and drop ports for a general nonreciprocal optical device, the circulator. We find that the two counterpropagating modes in the WGM microresonator couple to the quantum impurity with different coupling strengths due to the different dipole moments μ_+ and μ_-. For example, a Cs atom populated in $|6S_{1/2}, F = 4, m_F = 4\rangle$ results in $\mu_+ = \sqrt{45}\mu_-$ and $\mu_+ = \sqrt{25}\mu_-$ for a Rb atom populated in $|5\,^2S_{1/2}, F = 3, m_F = 3\rangle$. The quantum impurity strongly couples with the strength g_+- to the σ_+-polarized counterclockwise mode excited by the right-hand input photon. In contrast, it weakly interacts with the σ_--polarized clockwise mode driven by the left-hand input photon. The Hamiltonian describing the dynamics and interaction of the photons in the device has the form

$$\begin{aligned}\hat{H} = &\int dx\Big[\hat{C}_B^\dagger\Big(\omega_{\rm in} \mp i v_g\frac{\partial}{\partial x}\Big)\hat{C}_B \\ &+ V_1\delta(x)(\hat{a}^\dagger\hat{C}_B + \hat{C}_B^\dagger\hat{a})\Big] \\ &+ \int dx'\Big[\hat{C}_D^\dagger\Big(\omega_{\rm in} \pm i v_g\frac{\partial}{\partial x'}\Big)\hat{C}_D \\ &+ V_2\delta(x')\Big(\hat{a}^\dagger\hat{C}_D + \hat{C}_D^\dagger\hat{a}\Big)\Big] \\ &+ \delta(x)[g_\pm\hat{a}_c^\dagger\hat{S}_- + g_\pm^*\hat{S}_+\hat{a}_c) \\ &+ (\omega_c - i\kappa_i)\hat{a}_c^\dagger\hat{a}_c + (\omega_q - i\gamma_\pm)\hat{a}_e^\dagger\hat{a}_e,\end{aligned} \tag{B1}$$

where $\hat{C}_B^\dagger$ ($\hat{C}_D^\dagger$) is a bosonic operator creating the traveling mode in the bus (drop) waveguide; x and x' indicate the location in the bus waveguide and drop waveguide, respectively; V_1 (V_2) is the coupling strength between the bus (drop) waveguide and the cavity; and κ_i is the intrinsic decay rate of the cavity. $\gamma_\pm$ are the decay rates of the quantum impurity corresponding to the degenerate transition driven by the $\sigma_\pm$ polarization. For the left-hand input $\hat{C}_B^\dagger$, $\hat{a}_c^\dagger$ is the creation operator for the counterclockwise (σ_+) WGM mode, and $\hat{C}_D^\dagger$ is the bosonic operator creating a left-moving mode in the drop waveguide towards port P_4. For the right-hand input, $\hat{a}_c^\dagger$ creates the clockwise (σ_-) WGM mode and $\hat{C}_D^\dagger$ creates a right-moving mode going to the P_3 port.

Similar to the type-I diode, we have the eigenstate $|\psi\rangle = [\int dx\tilde{\phi}_B\hat{C}_B^\dagger + \int dx'\tilde{\phi}_D\hat{C}_D^\dagger + \tilde{e}_c\hat{a}_c^\dagger + \tilde{e}_a\hat{a}_e^\dagger\hat{a}_g]|\varnothing\rangle$ associated with the eigenvalue ω, where $\tilde{\phi}_B$ and $\tilde{\phi}_D$ are the wave packets of the traveling photons in the bus and drop waveguides, respectively. The slowly varying envelopes of the wave packets are given by $\tilde{\phi}_{B/D} = e^{-i\omega t}\phi_{B/D}$. We take $\phi_T(x) = e^{\pm iQx}[\theta(\mp x) + t_{\pm,B}\theta(\pm x)]$ and $\phi_D(x') = t_{\pm,D}e^{\mp iQx'}\theta(\mp x')$ [24]. Then the transmissions into the bus and drop waveguides are given by

$$t_{\pm,B}(\omega) = 1 + \frac{2i\kappa_{ex1}}{\omega_c - \omega - i\kappa - \frac{|g_\pm|^2}{\omega_q - \omega - i\gamma_\pm}}, \tag{B2a}$$

$$t_{\pm,D}(\omega) = \frac{2i\sqrt{\kappa_{ex1}\kappa_{ex2}}}{\omega_c - \omega - i\kappa - \frac{|g_\pm|^2}{\omega_q - \omega - i\gamma_\pm}}, \tag{B2b}$$

where $\kappa_{ex1}(\kappa_{ex2}) = V_1^2/2v_g(V_2^2/2v_g)$ is the decay rate of the cavity due to the external coupling $V_1(V_2)$ to the bus (drop) waveguide, and $\kappa = \kappa_i + \kappa_{ex1} + \kappa_{ex2}$ is the total decay rate of the cavity. We define the detuning $\Delta = \omega_c - \omega$ and always assume that $\omega_c = \omega_q$, the degenerate internal transition frequency of the V-type atom. The transmissions are defined as $T_{\pm,B} = |t_{\pm,B}|^2$ and $T_{\pm,D} = |t_{\pm,D}|^2$. Here we assume that the photons in both of the bus and drop waveguides have the same group velocity v_g.

[1] M.-C. Tien, T. Mizumoto, P. Pintus, H. Kromer, and J. E. Bowers, Opt. Express **19**, 11740 (2011).
[2] L. Bi, J. Hu, P. Jiang, D. H. Kim, G. F. Dionne, L. C. Kimerling, and C. A. Ross, Nat. Photonics **5**, 758 (2011).
[3] L. Fan, J. Wang, L. T. Varghese, H. Shen, B. Niu, Y. Xuan, A. M. Weiner, and M. Qi, Science **335**, 447 (2012).
[4] Y. Sun, Y. Wei Tong, C. Hua Xue, Y. Qiong Ding, Y. Hui Li, H. Jiang, and H. Chen, Appl. Phys. Lett. **103**, 091904 (2013).
[5] C. Wang, X.-L. Zhong, and Z.-Y. Li, Sci. Rep. **2**, 674 (2012).
[6] Z. Yu and S. Fan, Nat. Photonics **3**, 91 (2009).
[7] K. Fang, Z. Yu, and S. Fan, Phys. Rev. Lett. **108**, 153901 (2012).
[8] D.-W. Wang, H.-T. Zhou, M.-J. Guo, J.-X. Zhang, J. Evers, and S.-Y. Zhu, Phys. Rev. Lett. **110**, 093901 (2013).
[9] M. S. Kang, A. Butsch, and P. S. J. Russell, Nat. Photonics **5**, 549 (2011).
[10] A. Kamal, J. Clarke, and M. H. Devoret, Nat. Phys. **7**, 311 (2011).

[11] K. Xia, M. Alamri, and M. S. Zubairy, Opt. Express **21**, 25619 (2013).
[12] B. Peng, S. K. Özdemir, F. Lei, F. Monifi, M. Gianfreda, G. L. Long, S. Fan, F. Nori, and C. M. Bender, Nat. Phys. **10**, 394 (2014).
[13] C. E. Rüter, K. G. Makris, R. El-Ganainy, D. N. Christodoulides, M. Segev, and D. Kip, Nat. Phys. **6**, 192 (2010).
[14] H. J. Kimble, Nature (London) **453**, 1023 (2008).
[15] J. I. Cirac, P. Zoller, H. J. Kimble, and H. Mabuchi, Phys. Rev. Lett. **78**, 3221 (1997).
[16] Y. Shen, M. Bradford, and J.-T. Shen, Phys. Rev. Lett. **107**, 173902 (2011).
[17] M. Hafezi and P. Rabl, Opt. Express **20**, 7672 (2012).
[18] C. Junge, D. O'Shea, J. Volz, and A. Rauschenbeutel, Phys. Rev. Lett. **110**, 213604 (2013).
[19] D. O'Shea, C. Junge, J. Volz, and A. Rauschenbeutel, Phys. Rev. Lett. **111**, 193601 (2013).
[20] D. Witthaut and A. S. Sørensen, New J. Phys. **12**, 043052 (2010).
[21] F. Sedlmeir, M. Hauer, J. U. Fürst, G. Leuchs, and H. G. L. Schwefel, Opt. Express **21**, 23942 (2013).
[22] Q. A. Turchette, C. J. Hood, W. Lange, H. Mabuchi, and H. J. Kimble, Phys. Rev. Lett. **75**, 4710 (1995).
[23] X. Xu, B. Sun, P. R. Berman, D. G. Steel, A. S. Bracker, D. Gammon, and L. J. Sham, Nat. Phys. **4**, 692 (2008).
[24] J. T. Shen and S. Fan, Opt. Lett. **30**, 2001 (2005).
[25] K. Xia, Phys. Rev. A **89**, 023815 (2014).
[26] E. Prati, M. Hori, F. Guagliardo, G. Ferrari, and T. Shinada, Nat. Nanotechnol. **7**, 443 (2012).
[27] T. Aoki, B. Dayan, E. Wilcut, W. P. Bowen, A. S. Parkins, T. J. Kippenberg, K. J. Vahala, and H. J. Kimble, Nature (London) **443**, 671 (2006).
[28] E. E. Hach, III, A. W. Elshaari, and S. F. Preble, Phys. Rev. A **82**, 063839 (2010).
[29] M. Bradford and J.-T. Shen, Phys. Rev. A **85**, 043814 (2012).
[30] W.-B. Yan, J.-F. Huang, and H. Fan, Sci. Rep. **3**, 3555 (2013).
[31] D. E. Chang, A. S. Sørensen, E. A. Demler, and M. D. Lukin, Nat. Phys. **3**, 807 (2007).
[32] P. Kolchin, R. F. Oulton, and X. Zhang, Phys. Rev. Lett. **106**, 113601 (2011).
[33] J.-T. Shen and S. Fan, Phys. Rev. Lett. **98**, 153003 (2007).
[34] P. Longo, P. Schmitteckert, and K. Busch, Phys. Rev. Lett. **104**, 023602 (2010).
[35] J.-Q. Liao and C. K. Law, Phys. Rev. A **82**, 053836 (2010).
[36] T. Shi, S. Fan, and C. P. Sun, Phys. Rev. A **84**, 063803 (2011).
[37] B. Peropadre, J. Lindkvist, I.-C. Hoi, C. M. Wilson, J. J. Garcia-Ripoll, P. Delsing, and G. Johansson, New J. Phys. **15**, 035009 (2013).
[38] F. Benabid, P. J. Roberts, F. Couny, and P. S. Light, J. Europ. Opt. Soc. **4**, 09004 (2009).
[39] A. D. Slepkov, A. R. Bhagwat, V. Venkataraman, P. Londero, and A. L. Gaeta, Opt. Express **16**, 18976 (2008).
[40] G. Epple, K. S. Kleinbach, T. G. Euser, N. Y. Joly, T. Pfau, P. S. J. Russell, and R. Löw, Nat. Commun. **5**, 4132 (2014).
[41] P. S. Light, F. Benabid, F. Couny, M. Maric, and A. N. Luiten, Opt. Lett. **32**, 1323 (2007).
[42] J. Clarke, H. Chen, and W. A. van Wijngaarden, Appl. Opt. **40**, 2047 (2001). R. Thomas, C. Kupchak, G. S. Agarwal, and A. I. Lvovsky, Opt. Express **21**, 6880 (2013).
[43] J.-T. Shen and S. Fan, Phys. Rev. A **79**, 023837 (2009).
[44] J.-T. Shen and S. Fan, Phys. Rev. A **79**, 023838 (2009).